

Prediction of Horseshoe Chaos in Duffing-Van Der Pol Oscillator Driven By Different Periodic Forces

L. Ravisankar¹, V. Ravichandran², V. Chinnathambi³

^{1,2,3}(Department of Physics, Sri K.G.S. Arts College, Srivaikuntam-628619, Tamilnadu, India)

Abstract: An analytical threshold condition for the prediction of onset of horseshoe chaos is obtained in the Duffing-van der Pol oscillator driven by different periodic forces using the Melnikov method. The external periodic forces considered are sine wave, square wave, symmetric saw-tooth wave, rectified sine wave and modulus of sine wave. Melnikov threshold curve is drawn in a parameter space. Analytical predictions are demonstrated through direct numerical simulation. Numerical investigations including computation of stable and unstable manifolds of saddle and measuring the time elapsed between two successive transverse intersections are used to detect onset of horseshoe chaos.

Keywords – Duffing- van der Pol oscillator, Horseshoe chaos, Melnikov function, periodic forces, chaos

I. Introduction

Most of the previous works on the nonlinear oscillator systems employ excitations of the sinusoidal type only. It is of considerable interest to study the system under influence of nonsinusoidal excitation such as square wave, symmetric and asymmetric saw-tooth waves, rectified and modulus of sine waves. Recently many studies have shown that the effect of different kinds of periodic forcing on these systems is considerable and they can change the dynamical behaviours drastically. For example, onset of homoclinic chaos by a periodic string of pulses modulated by Jacobian elliptic function and periodic δ -function [1], generation of chaotic behavior by a distorted force [2], anti-control of chaos by certain periodic forces [3], suppression of chaos by δ -pulse [4], stochastic resonance, nonescape dynamics and occurrence of horseshoe chaos with different periodic forces [5-7] have been reported.

Horseshoe is the occurrence of transverse intersection of stable and unstable manifolds of a saddle fixed point in the Poincaré map and is a global phenomenon. Its appearance can be predicted analytically by employing the Melnikov technique [8]. This technique essentially gives a criterion for a transverse intersection of the stable and unstable manifolds of homoclinic / heteroclinic orbits which imply horseshoe chaos. Even though the orbits created by the horseshoe mechanism are unstable, global information can be obtained analytically using the Melnikov technique. The essence of this method is to calculate the so-called Melnikov integral, which can be used to predict the regions in the parameter space where Smale-horseshoe chaos occurs [8-10]. It is well known that the existence of horseshoe does not imply that trajectories will be asymptotically chaotic. The asymptotically chaotic motion is characterized by positive Lyapunov exponent. However, the orbits created by horseshoe mechanism display an extreme sensitive dependence on initial conditions and possibly exhibit either a chaotic transient before settling to stable orbits or a strange attractor [8]. In many dynamical systems [9,10] onset of chaos has been found to occur near the Melnikov-threshold curve. Consequently, the Melnikov-threshold curve is considered as a lower threshold for the onset of chaos.

The Melnikov technique was firstly applied by Holmes [11] to study the chaotic attractor of a periodically driven Duffing oscillator with negative linear stiffness. Recently, this method has been applied to certain nonlinear systems. Cao and Chen [12,13] studied control of homoclinic and heteroclinic bifurcations in double well and three- well oscillators by a second sinusoidal forces. Nbenjo et al [14] analysed the control of escape and horseshoe chaos in a harmonically excited particle from a catastrophic single-well four-well potential. Dana et al [15] reported experimental evidence of shil'nikov-type homoclinic chaos in asymmetry induced Chua's oscillator. Tang et al [16] studied the relationship between the order of chaos of Melnikov function and the harmonic components of a system. Threshold values of chaotic motion under the periodic and quasiperiodic perturbation in Duffing and Duffing-van der Pol oscillators are obtained by Melnikov method [17, 18]. Rajasekar et al [19, 20] investigated the possibility of controlling horseshoe and asymptotic chaos in the Duffing-van der Pol oscillator using Melnikov method. Effect of bounded noises has also been studied in certain oscillators [21-25].

In this paper we study both analytically and numerically the effect of the shape of periodic forces on horseshoe chaos in Duffing-van der Pol oscillator equation

$$\ddot{x} + p\dot{x}(1-x^2) - \alpha^2 x + \beta x^3 = F(t) \quad (1)$$

The motivation for our interest in this system is that it has wide range of applications in physics and biology. Eq. (1) is an alternative form of Bonhoeffer-van der Pol oscillator [26, 27] driven magnetic oscillator [28] and also describe the dynamics of charged density in the plasma of a rf gas discharge. Recently, Ravichandran et al [29] studied the effect of the shape of periodic forces and second periodic forces on horseshoe chaos in Duffing oscillator. Our objective here is to explore the possibility of occurrence of horseshoe chaos using both analytical and numerical techniques. In our present analysis we use Melnikov analytical method to study the influence of shape of periodic forces on homoclinic orbits.

The paper is organized as follows. In section 2 we obtain the Melnikov threshold condition for the transverse intersection of homoclinic orbits for the system (1) separately for each of the periodic forces. In section 3 the effect of shape of periodic forces on horseshoe dynamics is analyzed using the Melnikov method. The analytical predictions is demonstrated through direct numerical simulations. Controlling of asymptotic chaos is also studied. Finally, section 4 contains the concluding remarks.

II. Preliminaries And Calculation Of Melnikov Function

We consider the linearly perturbed double-well Duffing-van der Pol (DVP) oscillator driven by an external periodic force $F(t)$ in the form

$$\dot{x} = y, \quad (2a)$$

$$\dot{y} = \alpha^2 x - \beta x^3 + \varepsilon[-p x(1-x^2) + F(t)], \quad (2b)$$

where $F(t)$ is an external periodic force, ε is a small parameter, $\alpha^2 > 0$ and $\beta > 0$. Figure 1 depicts various periodic forces considered in our present work. The unperturbed part of the system (2) ($\varepsilon=0$) has one saddle point $(x^*, y^*) = (0,0)$ and two centre type fixed points $(x^*, y^*) = (\pm\alpha/\sqrt{\beta}, 0)$. The two homoclinic orbits connecting the saddle to itself are given by

$$W^\pm(x_h(t), y_h(t)) = (\pm\alpha\sqrt{2/\beta} \sec \alpha t, \mp\alpha^2\sqrt{2/\beta} \sec \alpha t \tanh \alpha t), \quad \tau = t - t_0 \quad (3)$$

Stable manifolds (W_s^\pm) and unstable manifolds (W_u^\pm) of homoclinic orbits are indicated in Fig. 2.

Periodic orbits are nested within and outside the homoclinic orbits. For $\varepsilon = 0$, the stable and unstable branches of homoclinic orbits join smoothly. When the dissipative perturbation is included the stable manifold W_s^\pm and unstable manifold W_u^\pm do not join. However, above certain critical amplitude of the external periodic force transverse intersections of W_s^\pm and W_u^\pm occurs. The presence of such intersections implies that the Poincaré map

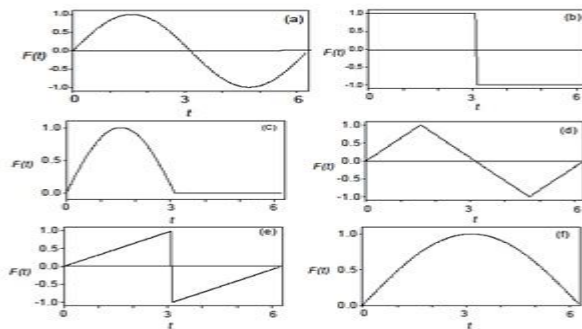


Figure 1: Wave form of various periodic forces (a) sine wave (b) square wave (c) rectified sine wave (d) symmetric saw-tooth wave (e) asymmetric saw-tooth wave and (f) modulus of sine wave. For all the forces period is $2\pi/\omega$, $\omega = 1$ and amplitude f is 1.

has the so-called horseshoe chaos [8, 30]. Eventhough the orbits created by the horseshoe mechanism are unstable they can exert a dramatic influence on the behavior of orbits which pass close to the point of intersection. The appearance of transverse intersections of homoclinic orbits can be predicted analytically by the Melnikov technique. In order to apply the Melnikov technique, in general, we rewrite the given equation of motion into the following standard form

$$\dot{x} = f_1(x, y) + \varepsilon g_1(x, y, t) \quad (4a)$$

$$\dot{y} = f_2(x, y) + \varepsilon g_2(x, y, t) \quad (4b)$$

where g_1 and g_2 are periodic in t with period T , the Melnikov function is given by [30]

$$M(t_0) = \int_{-\infty}^{+\infty} f(X_h(\tau)) \wedge g(X_h(\tau), t) \exp\left[-\int_0^T \text{trace}[D_X f(X_h(S))] ds\right] d\tau \quad (5)$$

where $X_h = (x_h, y_h)$ represents homoclinic orbits of the unperturbed systems, $f \wedge g = f_1 g_2 - f_2 g_1$ and D_X denotes the partial derivatives with respect to $X = (x, y)$.

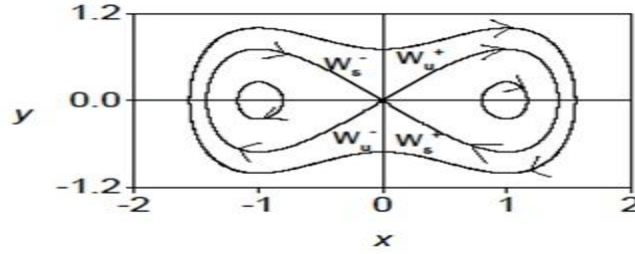


Figure 2: Phase trajectories of the unperturbed system. The stable (W_s^\pm) and unstable manifold (W_u^\pm) parts of homoclinic orbits connecting saddle to itself are indicated. The analytical expression for the homoclinic orbits is given by Eq. (3).

For the DVP Eq. (2) the Melnikov function is

$$M(t_0) = \int_{-\infty}^{+\infty} y_h [-p y_h (1 - x_h^2) + F(\tau + t_0)] d\tau. \quad (6)$$

In the following we calculate the Melnikov function for the system (2) with different periodic forces.

Sine wave

For the system (2) driven by the force $F(t) = f_{\sin} \sin \omega t$, the Melnikov integral is worked out as

$$M_{\sin}^\pm(t_0) = A \pm f_{\sin} B \cos \omega t_0 \quad (7a)$$

where

$$A = \frac{4p\alpha^3}{3\beta} \left[1 - \frac{4\alpha^2}{5\beta} \right], \quad B = \sqrt{\frac{2}{\beta}} \pi \omega \sec h \left(\frac{\pi \omega}{2\alpha} \right) \quad (7b)$$

Square wave

For the square wave $F(t) = F_{sq}(t + 2\pi/\omega) = f_{sq} \operatorname{sgn}(\sin \omega t)$ where $\operatorname{sgn}(y)$ is sign of y . The Fourier series is

$$F_{sq}(t) = \frac{4f}{\pi} \sum_{n=1}^{\infty} \frac{\sin(2n-1)\omega t}{(2n-1)} \quad (8a)$$

Using its Fourier series we obtain

$$M_{sq}^{\pm}(t_0) = A \pm f_{sq} \sum_{n=1}^{\infty} B_n \cos(2n-1)\omega t_0 \quad (8b)$$

where

$$B_n = \frac{4\sqrt{2}\omega}{\sqrt{\beta}} \operatorname{sech} h \left[\frac{\pi(2n-1)\omega}{2\alpha} \right] \quad (8c)$$

Symmetric saw-tooth wave

The numerical implementation of the force is given by

$$F_{sst}(t) = \begin{cases} \frac{4f_{sst}t}{T}, & 0 \leq t \leq \pi/2\omega, \\ -\frac{4f_{sst}t}{T}, & \pi/2\omega \leq t \leq 3\pi/2\omega, \\ \frac{4f_{sst}t}{T} - 4f_{sst}, & 3\pi/2\omega \leq t \leq 2\pi/\omega, \end{cases} \quad (9a)$$

where T is the period of the force and t is taken as mod $2\pi/\omega$. Its Fourier series

$$F_{sst}(t) = \frac{8f}{\pi^2} \sum_{n=1}^{\infty} \frac{(-1)^{(n+1)} \sin(2n-1)\omega t}{(2n-1)^2}. \quad (9b)$$

The Melnikov function is

$$M_{sst}^{\pm}(t_0) = A \pm f_{sst} \sum_{n=1}^{\infty} B_n \cos(2n-1)\omega t_0 \quad (9c)$$

where

$$B_n = \frac{8\sqrt{2}\omega}{\pi\sqrt{B}} \frac{(-1)^{n+1}}{(2n-1)} \operatorname{sech} h \left[\frac{\pi(2n-1)\omega}{2\alpha} \right] \quad (9d)$$

Asymmetric saw-tooth wave

For the asymmetric saw-tooth wave,

$$F_{ast}(t) = F_{ast}\left(t + \frac{2\pi}{\omega}\right) = \begin{cases} \frac{2f_{ast}t}{T}, & 0 \leq t \leq \pi/\omega, \\ \frac{2f_{ast}t}{T} - 2f_{ast}, & \pi/\omega \leq t \leq 2\pi/\omega, \end{cases} \quad (10a)$$

where t is taken as mod $2\pi/\omega$. The Fourier series of $F_{ast}(t)$ is given by

$$F_{ast}(t) = \frac{2f}{\pi} \sum_{n=1}^{\infty} \frac{(-1)^{n+1} \sin n\omega t}{n} \quad (10b)$$

We obtain

$$M_{ast}^{\pm}(t_0) = A \pm f_{ast} \sum_{n=1}^{\infty} B_n \cos n\omega t_0 \quad (10c)$$

where

$$B_n = \frac{2\sqrt{2}\omega}{\sqrt{\beta}} (-1)^{n+1} \sec h \left[\frac{n\pi\omega}{2\alpha} \right] \quad (10d)$$

Rectified sine wave

For the rectified sine wave

$$F_{rec}(t) = F_{rec}(t + 2\pi/\omega) = \begin{cases} f_{rec} \sin \omega t, & 0 \leq t \leq \pi/\omega \\ 0, & \pi/\omega \leq t \leq 2\pi/\omega \end{cases} \quad (11a)$$

The Fourier series of rectified sine wave is

$$F_{rec}(t) = \frac{f_{rec}}{\pi\omega} + \frac{2f_{rec}\omega}{\pi} \sum_{n=1}^{\infty} \frac{1}{\omega^2 - n^2} \cos n\omega t \quad (11b)$$

for $0 < t < \pi/\omega$ and 0 for $\pi/\omega < t < 2\pi/\omega$

The Melnikov function is

$$M_{rec}^{\pm}(t_0) = -A \pm 2f_{rec} \sum_{n=1}^{\infty} B_n C_n \sin n\omega t_0 \quad (11c)$$

where

$$B_n = \frac{2\omega\alpha^2}{\pi} \sqrt{\frac{2}{\beta}} \frac{1}{(\omega^2 - n^2)} \quad (11d)$$

and

$$C_n = \int_{(2n-2)\pi/\omega}^{(2n-1)\pi/\omega} \sec h\alpha\tau \tanh\alpha\tau \sin n\omega\tau d\tau \quad (11e)$$

C_n can be evaluated numerically.

Modulus of sine wave

For the modulus of sine wave

$$F_{msw}(t) = F_{msw}(t + 2\pi/\omega) = f_{msw} \sin(\omega t/2) \quad (12a)$$

Its Fourier series is

$$F_{msw}(t) = \frac{2f}{\pi} - \frac{4f}{\pi} \sum_{n=1}^{\infty} \frac{n \cos n\omega t}{(4n^2 - 1)} \quad (12b)$$

Melnikov function is

$$M_{msw}^{\pm}(t_0) = A \pm f_{msw} B \cos \left(\frac{\omega t_0}{2} \right) \quad (12c)$$

where

$$B = \frac{\pi\omega}{\sqrt{2\beta}} \sec h \left(\frac{\pi\omega}{4\alpha} \right) \quad (12d)$$

III. Effect of Shape Of Periodic Forces On Horseshoe Chaos

In this section we compute the Melnikov threshold values for the onset of horseshoe chaos and compare it with numerical predictions. For the sine wave, the condition for transverse intersection of stable and unstable manifolds is

$$|f_{\sin}| \geq |f_m| = \frac{2\sqrt{2}p\alpha^3 \left(1 - \frac{4\alpha^2}{5\beta}\right)}{3\pi\omega\sqrt{\beta}} \operatorname{cosh}\left(\frac{\pi\omega}{2\alpha}\right) \quad (13)$$

Eq. (13) is the necessary condition for the occurrence of horseshoe chaos. The sufficient condition requires the existence of simple zeros of $M(t_0)$. Equality sign in Eq. (13) corresponds to tangential intersection. For other forces except sine and modulus of sine waves we can not write the sufficient condition for the existence of simple zeros of $M(t_0)$ as like Eq. (13) since $M(t_0)$ is a convergent series. However, the occurrence of homoclinic bifurcation can be studied by measuring the time τ_M elapsed between two successive zeros of $M(t_0)$. We consider sufficiently large number of terms say, 50 terms in the summation of the equation

for $M(t_0)$. For a fixed value f , t_0 is varied from 0 to $200T$ where $T = \frac{2\pi}{\omega}$ is period of the external force.

If the sign of $M(t_0)$ remains same in this time interval then there is no zero of $M(t_0)$ and τ_M is assumed as

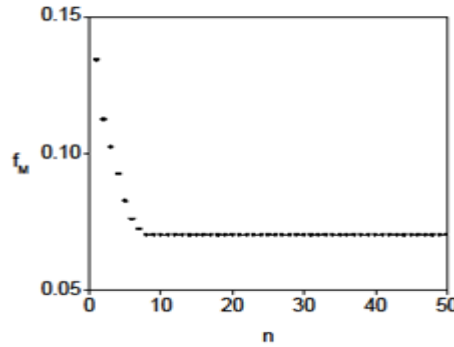


Figure 3: f_M versus n , the number of terms in the summation in Eq. (8b) for $\alpha = 1$, $\beta = 5.0$, $p = 0.4$ and $\omega = 1$ when the system (1) is driven by the square wave force. Variation in f_M converges to a constant value with increase in n .

infinity. τ_M is calculated for a range of amplitude of the external force. The value of f , at which first time $M(t_0)$ changes sign and thereby giving finite τ_M is the Melnikov threshold value for homoclinic bifurcation. Figure 3 shows the plot of f_m versus n , the number of terms in the summation in Eq. (8b) for the square wave force. f_m converges to a constant value with increase in n . For $n > 10$, the variation in f_m is negligible. Similar result is found for the other forces also. In our numerical calculation of f_m we fix $n = 50$. Figure 4 shows the variation of $1/\tau_M$ versus f for the system (2) driven by different periodic forces. Solid curve represents the inverse of first intersection time, $1/\tau_M$ of stable and unstable branches of homoclinic orbits W^+ . Dashed curve corresponds to the orbit W^- . Horseshoe chaos does not occur when $1/\tau_M$ is zero and it occurs in the region where $1/\tau_M > 0$. Figure 5 shows the plot of the threshold curve for horseshoe chaos in the $(f - \omega)$ parameter plane. Below the threshold curve no transverse intersection of stable and unstable manifolds of the saddle occurs and above the threshold curve the transverse intersection of the orbits of the saddle occurs. This figure clearly illustrates the effect of the various forces. Smooth variation of f_m is found for all the forces. The threshold curves are non-intersecting except rectified and modules of sine wave forces. The variation of f_m with ω is similar for all the periodic forces. Among the six forces f_m is maximum for the rectified sine wave and minimum for the square wave. Thus onset of horseshoe chaos can be either delayed or advanced by an appropriate choice of periodic force.

We verify the analytical predictions by numerically computing the stable and unstable manifolds of the saddle. The unstable manifolds are obtained by numerically integrating the Eq. (2) by the fourth-order Runge

Kutta method in the forward time for a set of 900 initial conditions chosen around the perturbed saddle point. The stable manifolds are obtained by integrating the equation of motion in reverse time. In Fig. 6 we plotted the orbits of the saddle for two values of f for the forces-one for $f < f_m$ and another for $f > f_m$. For clarity only part of the manifolds are shown. In the left-side sub plots, the stable and unstable orbits are well separated. In the right-side subplots for $f > f_m$, we can clearly notice transverse intersection of orbits at certain places.

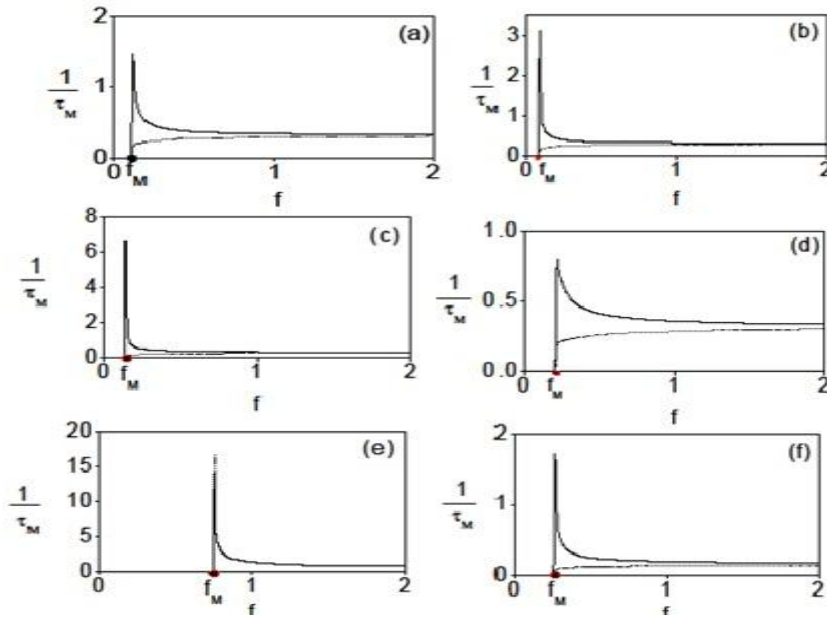


Figure 4: Variation of $1/\tau_M$ versus f for the system (1) driven by the forces (a) sine wave (b) square wave (c) symmetric saw-tooth wave (d) asymmetric saw-tooth wave (e) rectified sine wave and (f) modulus of sine wave. The values of the other parameters in Eq. (1) are $\alpha = 1$, $\beta = 5.0$, $p = 0.4$ and $\omega = 1$. Continuous curve is for positive sign and dashed curve is for negative sign of $M(t_0)$.

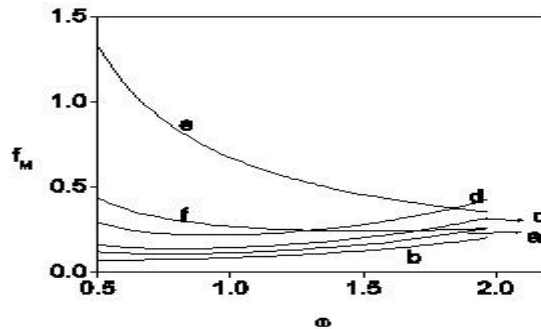


Figure 5: Melnikov threshold curves for horseshoe chaos in the $(f - \omega)$ plane for the system (1) driven by the forces (a) sine wave (b) square wave (c) symmetric saw-tooth wave (d) asymmetric saw-tooth wave (e) rectified sine wave and (f) modulus of sine wave. The values of the other parameters in Eq. (1) are $\alpha = 1$, $\beta = 5.0$, $p = 0.4$ and $\omega = 1$.

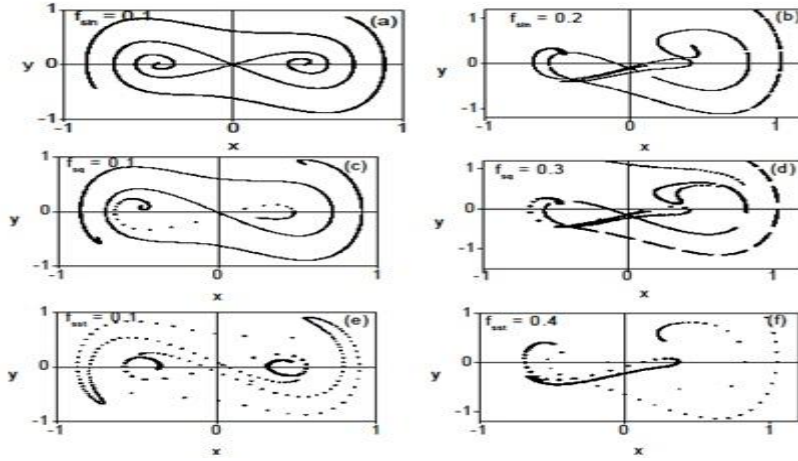


Figure 6: Numerically computed stable and unstable manifolds of the saddle fixed point of the system (1). The system is driven by (a-b) sine wave (c-d) square wave (e-f) symmetric saw-tooth wave (g-h) asymmetric saw-tooth wave (i-j) rectified sine wave and (k-l) modulus of sine wave. The values of the other parameters in Eq.(1) are $\alpha = 1$, $\beta = 5.0$, $p = 0.4$ and $\omega = 1$. Left side subplots are for $f < f_M$ while the right side subplots are for $f > f_M$.

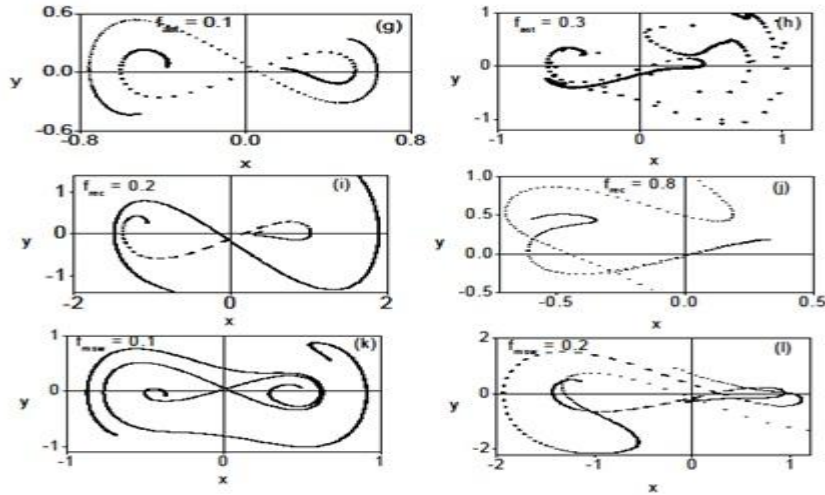


Figure 6 : continued...

IV. CONCLUSION

In the present paper we considered the Duffing-van der Pol oscillator driven by different periodic forces. We studied the effect of the shape of periodic forces on horseshoe chaos. Applying Melnikov analytical method, we obtained the threshold condition for onset of horseshoe chaos, that is, transverse intersections of stable and unstable branches of homoclinic orbits. Melnikov threshold curve is drawn in a parameter space. Among the six forces, f_m is maximum for the rectified sine wave force and is minimum for the square wave. Analytical prediction of horseshoe chaos is found to be in good agreement with numerical simulation for all the forces. With the good agreement obtained between theoretical and numerical predictions we emphasize that the Melnikov analysis can be successfully used to predict the onset of chaos in the presence of weak periodic perturbation.

References

- [1] R. Chacon, Chaos and geometrical resonance in the damped pendulum subjected to periodic pulses, *J. Math. Phys.* 38, 1997, 1477-1483
- [2] K. Konishi, Generating chaotic behaviours in an oscillator driven by periodic forces, *Phys. Lett. A.*, 320, 2003, 200-206
- [3] Z.M. Ge and W.Y. Leu, Anti-control of chaos of two degrees of freedom loud speaker and synchronization of different order systems, *Chaos, Solitons and Fractals*, 20, (2004), 503-521
- [4] A.Y.T. Leung and L. Zengrong, Suppressing chaos for some nonlinear oscillators, *Int. J. Bifur. and Chaos* 14, 2004, 1455-1465
- [5] V.M. Gandhimathi, K. Murali and S. Rajasekar, Stochastic resonance with different periodic forces in overdamped two coupled anharmonic oscillators, *Chaos, Solitons and Fractals*, 30, 2006, 1034-1047
- [6] V. Ravichandran, V. Chinnathambi and S. Rajasekar, Study of nonescape dynamics in Duffing oscillator with four different periodic forces, *Indian Journal of Physics*, 86(10), 2012, 907-911
- [7] V. Ravichandran, V. Chinnathambi and S. Rajasekar, Effect of rectified and modulated sine forces on chaos in Duffing oscillator, *Indian J. Phys.*, 83(11), (2009) 1593-1603
- [8] J. Guckenheimer and P. Holmes, *Nonlinear oscillations, Dynamical system and bifurcations of vector fields* (Springer-Verlag, 1983, New York)
- [9] M. Bartuccelli, P.L. Christiansen, N.F. Pedersen and M.P. Soersen, Prediction of Chaos in Josephson junction by the Melnikov function, *Phys. Rev. B*, 33, 1986, 4686-4691
- [10] M. Bartuccelli, P.L. Christiansen, N.F. Pedersen and M. Salerno, Horseshoe chaos in the space-independent double sine-Gordon, *Wave Motion*, 8, 1986, 581-594
- [11] P.J. Holmes, A nonlinear oscillator with a strange attractor, *Philos trans R Soc*, A292, 1979, 418-48
- [12] H. Cao, Primary resonant optimal control for homoclinic bifurcations in single-degree-of-freedom nonlinear oscillators, *Chaos, Solitons and Fractals*, 24, 2005, 1387-1398
- [13] H. Cao and G. Chen, Global and local control of homoclinic and heteroclinic bifurcations, *Int. J. Bifur. and Chaos*, 15, 2005, 2411-2432
- [14] B.R.N. Nbandjo, Y. Salissou, P. Wofo, Active control with delay of catastrophic motion and horseshoe chaos in a single-well Duffing oscillator, *Chaos, Solitons and fractals*, 23, 2005, 809-816
- [15] S.K. Dana, S. Chakraborty and G. Ananthakrishna, Homoclinic bifurcation in Chua's circuit, *Pramana J. of Phys.*, 64, 2005, 443-454
- [16] Y. Tang, F. Yang, G. Chen and T. Zhou, Classification of homoclinic tangencies for periodically perturbed systems, *Chaos, Solitons and Fractals*, 28, 2006, 76-89
- [17] Z. Zing and R. Wang, Complex dynamics in Duffing system with two external forcings, *Chaos, Solitons and Fractals*, 23, 2005, 399-411
- [18] Z. Zing, Z. Yang and T. Jiang, Complex dynamics in Duffing-Van der Pol equation, *Chaos, Solitons and Fractals*, 27, 2006, 722-747
- [19] S. Rajasekar, Controlling of chaos by weak periodic perturbations in Duffing oscillator, *Pramana J. of Phys.*, 41, 1993, 295-309
- [20] S. Rajasekar, S. Parthasarathy, and M. Lakshmanan, Prediction of horseshoe chaos in BVP and DVP oscillators, *Chaos, Solitons and Fractals*, 2, 1992, 271-280
- [21] W.Y. Liu, W.Q. Zhu and Z.L. Huang, Effect of bounded noise on chaotic Duffing oscillator under parametric excitation, *Chaos, Solitons and Fractals*, 12, 2001, 527-537
- [22] Z.H. Liu, W.Q. Zhu, Homoclinic bifurcation and chaos in simple pendulum under bounded noise excitations, *Chaos, Solitons and Fractals*, 20, 2004, 593-607
- [23] X. Yang, W. Xu and Z. Sun, Effect of bounded noise on the chaotic motion of a Duffing-van der Pol oscillator in a Φ^6 potential, *Chaos, Solitons and Fractals*, 27, 2006, 778-788
- [24] X. Yang, W. Xu, Z. Sun and T. Fang, Effect of bounded noise on chaotic motion of a triple-well potential system, *Chaos, Solitons and Fractals*, 25, 2005, 415-424
- [25] W.Q. Zhu and Z.H. Liu, Homoclinic bifurcation and chaos in coupled simple pendulum and harmonic oscillator under bounded noise excitation, *Int. J. Bifur. Chaos*, 15, 2005, 233-243
- [26] S. Rajasekar and M. Lakshmanan, Controlling of chaos in BVP oscillator, *Int. J. Bifur. Chaos*, 2, 1992, 201-204
- [27] S. Rajasekar and M. Lakshmanan, Algorithms for controlling chaotic motion: application for the BVP oscillator, *Physica D* 67, 1993, 282-300
- [28] K. Wiesenfeld and B. McNamara, Small-signal amplification in bifurcating dynamical systems, *Phys. Rev. A*, 33, 1986, 629-642
- [29] V. Ravichandran, V. Chinnathambi and S. Rajasekar and C.H. Lai, arxiv:0808.0406v1 [nlin.CD] Aug.2008
- [30] S. Wiggins *Global bifurcations and Chaos* (Springer, Berlin, 1988)